

Article

Projections of Cause-Specific Mortality and Demographic Changes under Climate Change in the Lisbon Metropolitan Area: A Modelling Framework

Mónica Rodrigues

Centre of Studies on Geography and Spatial Planning, Department of Geography and Tourism,
University of Coimbra, 3004-530 Coimbra, Portugal; monica.a.rodrigues@hotmail.com

Abstract: Climate change and related events, such as rising temperatures and extreme weather, threaten population health and well-being. This study quantified the impact of climate change on temperature-related, cause-specific mortality while considering adaptations and future demographic changes in Lisbon Metropolitan Area, Portugal. A distributed lag non-linear model (DLNM) was applied to quantify the burden of temperature-related mortality during the present (or reference, 1986–2005) scenario and a future scenario (2046–2065). There was an increase of 0.33% in temperature-related excess mortality (95% CI: 0.02 to 0.59) and significantly lower all-cause deaths in the future. These measurements were attributable to extreme cold and considered an adaptation threshold of 1 °C with no population changes, resulting in an estimated net difference of –0.15% (95% CI: –0.26 to –0.02), a threshold of 1 °C with a high population scenario of –0.15% (95% CI: –0.26 to –0.01), and a threshold of 1 °C with a low population scenario of –0.15% (95% CI: –0.26 to –0.01). Moderate cold exposure under a threshold of 1 °C and a high population scenario reduced future temperature-related deaths and diabetes mellitus (–1.32, 95% CI: –2.65 to 0.23). Similarly, moderate heat exposure under a threshold of 4 °C and a high population scenario had the highest increase in net changes (6.75, 95% CI: –5.06 to 15.32). The net difference in AF% was due to ischemic heart disease, which was the highest for moderate heat exposure with an adaptation threshold of 4 °C only. It decreased slightly with increasing adaptation levels. The most significant increase in net differences for temperature-related excess deaths occurred in respiratory diseases and was associated with heat. A significant decline in net differences was also observed in excess cold-related deaths due to respiratory disease. These findings contribute to the discussion of how climate change impacts human health. Furthermore, they can help guide and monitor adaptation policies in response to climate change.

Keywords: cause-specific mortality; population; climate change; projections; distributed lag non-linear model (DLNM); WRF model; Portugal



Citation: Rodrigues, M. Projections of Cause-Specific Mortality and Demographic Changes under Climate Change in the Lisbon Metropolitan Area: A Modelling Framework. *Atmosphere* **2023**, *14*, 775. <https://doi.org/10.3390/atmos14050775>

Academic Editor: Tanja Cegnar

Received: 21 February 2023

Revised: 10 April 2023

Accepted: 23 April 2023

Published: 24 April 2023



Copyright: © 2023 by the author. Licensee MDPI, Basel, Switzerland. This article is an open access article distributed under the terms and conditions of the Creative Commons Attribution (CC BY) license (<https://creativecommons.org/licenses/by/4.0/>).

1. Introduction

Studies have reported that global climate change threatens population health and well-being, particularly exposure to heat and cold events [1–12]. Extreme temperatures, such as heat events, have been well documented [13–24]. For example, a study by Vicedo-Cabrera et al. [22] demonstrates a considerable temperature increase over time and frequent extreme weather events, such as heatwaves. The frequency, intensity, and duration of extreme temperature events will increase, according to the Intergovernmental Panel on Climate Change [2,23] and the World Health Organization [25]. Urbanisation and the increasing incidence of chronic conditions primarily cause vulnerability to extreme heat. Disadvantaged and marginalised groups are particularly affected [1,26–33]. Most studies project that future increases in heat-related deaths will outweigh those due to cold [34,35]. Several countries have shown reduced winter mortality due to milder winters [12,36,37]. Portugal's temperature-attributable mortality projections

are mostly related to total or non-accidental mortality. However, few data on temperature-related cause-specific mortality are available, which limits our knowledge of climate change effects on specific conditions, including health determinants. Based on RCP8.5 (Representative Concentration Pathways) greenhouse gas emissions scenario, metropolitan-specific climate projections for two 20-year periods, 1986–2005 and 2046–2065, were used considering low, medium, and high population scenarios to estimate the future impact of climate change on temperature-related, cause-specific mortality.

2. Materials and Methods

2.1. Overview

This study was conducted in the Lisbon Metropolitan Area (LMA), Portugal. LMA comprises 18 municipalities in Portugal's south-central region. It represents the main social and demographic centre of the country. According to the latest census conducted in 2021, the LMA has a population of 2,871,133. The LMA was selected for this study because of its vulnerability to extreme weather and temperature events, which have significantly impacted vulnerable populations [14,38].

2.2. Data Sources

2.2.1. Mortality Data

Daily data on cause-specific deaths in the LMA were obtained from Statistics Portugal (INE) for 1986–2005.

Causes of death were coded according to the International Classification of Diseases, ninth revision (ICD-9) and tenth revision (ICD-10), as follows: diabetes mellitus (ICD-9: 250 code series; ICD-10: E10-E14); ischemic heart diseases (ICD-9: 410–414; ICD-10: I20-I25); cerebrovascular diseases (ICD-9: 430–438; ICD-10: I60-I69); and respiratory diseases (ICD-9: 460–519; ICD-10: J00-J99). During this period, diabetes mellitus (DM) caused 16,447 deaths; ischemic heart disease (HD) caused 64,618 deaths; cerebrovascular disease (CVD) caused 91,824 deaths; and respiratory diseases (RD) caused 37,422 deaths.

2.2.2. Temperature Projections

Projections of historical and future temperatures for the LMA were obtained from the Weather Research and Forecasting model (WRF). This model was used to dynamically downscale climate data from the Max Planck Institute for Meteorology Earth System Model (MPI-ESM) to a higher horizontal resolution (9 Km) climate grid. It is recognised as one of the most robust climate simulation models [17,25].

RCP8.5 greenhouse gas emissions [39] were used as a reference for the current climate (1986–2005) and to simulate projections for the mid-term climate (2046–2065). The average, maximum, and minimum near-surface (2 m high) daily atmospheric temperatures for each location and climate were extracted for the LMA using the closest grid point in the model [17]. The simulated data used in this study were previously validated [40]. Various studies have used these simulations to evaluate different climate aspects [17,41].

2.2.3. Population Data

Population estimates for the historical period (1986–2005) and projected future population estimates (2046–2065) were obtained from Statistics Portugal (INE—Portuguese National Institute of Statistics). According to INE, three fertility hypotheses were defined: 'low', which considers a low fertility hypothesis, medium mortality hypothesis, and low migration hypothesis; 'medium', which considers medium fertility, mortality, and migration hypotheses; and 'high', resulting from high evolution hypotheses for fertility, mortality, and migration.

2.3. Data Analysis

2.3.1. Estimation of Temperature–Mortality Relationships

Based on a previous study, a distributed lag non-linear model (DLNM) [42–45] was used with a 21-day lag to quantify the relationship between daily temperature and mortality, as well as mortality and lag days [46]. Assuming that daily cause-specific deaths (Y_t) follow a quasi-Poisson distribution, the model is of the form

$$Y_t \sim \text{quasiPoisson}(\mu_t)$$

$$\mu_t \equiv E(Y_t)$$

$$\log E[Y_t] = \alpha + \log(\text{POP}_t) + \delta_1 \text{DOW}_t + \delta_2 \text{HOY}_t + \delta_3 \text{SEASON}_t + \text{ns}(\text{RH}) + \text{ns}(\text{TIME}_t) + \text{cb}(x_{t-l}, \beta_l)$$

where $\log(\text{POP}_t)$ represents the logarithm of the population (POP) used to scale the modelling of the mean mortality count; days of the week (DOW), holiday (Hoy), and SEASON (Winter, Summer, and others) are fixed effects; and ns(RH) is the natural cubic spline for relative humidity, with 3 degrees of freedom (df). The model also includes a natural cubic spline with 8 df per year to adjust for long-term trends and seasonal mortality in the data.

To examine the non-linear and lag effects of temperature on mortality, a cross-basis function $\text{cb} = \int_{l_0}^{21} f \cdot w(x_{t-l}) dl \approx \sum_{l=l_0}^{21} f \cdot w(x_{t-l}, l) = w_{x,t}^T$ involving a tensor product between the basis chosen for the temperature–mortality function, $f(x)$, and lag–mortality function, $w(l)$, was employed. A flexible quadratic B-spline function was used to model the cross-basis term $\text{cb}(x_{t-l}, \beta_l)$, accounting for 21 days of lag. Three internal knots were placed at the 10th, 75th, and 90th percentiles of the temperature distribution and log scale for the lag dimension (up to 21 days).

The exposure–lag–response association was considered a relative risk (RR) for the minimum mortality temperature. Mild and extreme cold temperatures ranged from the minimum mortality temperature (MMT) to the 1st percentile and below the 1st percentile of the temperature distribution, respectively. Mild and extreme heat temperatures ranged from the MMT to the 99th percentile and above the 99th percentile of the temperature distribution, respectively. This selection was determined according to several epidemiological studies [47].

2.3.2. Projections of Exposure–Response Relationships and Attributable Mortality Rates

The strategy for projecting temperature–mortality associations was motivated by previous studies [48,49]. We extrapolated the temperature–mortality curve for the historical period with projected temperatures for the future period. We assumed that future mortality trends resemble the historical annual series. Furthermore, Golsing et al. [50] recommended two adaptation types. Temperature threshold shifts and exposure–response function (ERF) slope reductions were also explored. We estimated these temperature–mortality relationships, backwards attributable fractions (AF) and attributable number (AN) due to non-optimal temperatures (below and above MMT), using the overall cumulative temperature–mortality association and the RR corresponding to daily temperatures (below or above MMT) for each lag day.

$$AF_{x,t} = 1 - e^{-\sum_{l=l_0}^L \beta_{x_{t-l}}}$$

$$AN_{x,t} = AF_{x,t} \cdot n_t$$

The parameter β represents $\log(\text{RR})$, the logarithm of risks associated with temperature exposure, and n_t is the number of deaths at time t . The total attributable number (AN) of heat-related deaths corresponds to summing the subsets of days with temperatures above MMT, while days with temperatures below MMT are summed for cold-related deaths.

Similarly, the total AF net differences due to hot and cold temperatures were explored. By comparing excess mortality in the future to the historical period, we estimated the net effect of temperature-related mortality over time. Additionally, a series of sensitivity analyses were conducted to examine the robustness of the results to the model specification.

All data analyses in this study were conducted in R software (version 4.1.0), using package “dlnm”. A detailed explanation of “dlnm” is described in Gasparrini et al. [43].

3. Results

3.1. Exploratory Data Analysis

Table 1 presents the distribution of the key variables considered in this study. During the historical period (1986–2005), a high proportion of deaths were due to cerebrovascular disease (CVD), with a daily mean (SD) of 12.57 (4.53) and 91,824 total deaths compared to other cause-specific deaths (Table 1). The mean daily minimum and maximum temperatures for the same period were 13.43 °C and 18.52 °C, respectively. The mean daily temperature ranged from 3.4 °C to 34.7 °C, and its interquartile range was 12.5 °C–19.3 °C. For future projected temperatures (all year), the mean daily minimum and maximum temperatures for the projected period were 14.9 °C and 20.5 °C, respectively (Table 1). The mean daily projected temperature ranged from 5.6 °C to 34.6 °C, and its interquartile range was 13.8 °C–21.2 °C.

Table 1. Descriptive summaries of daily cause-specific mortality count and meteorological variables for the historical (1986–2005) and future (2046–2065) periods.

Variables	Total	Mean	SD	Min	Max	Quantiles				
						1	25	50	75	99
1986–2005										
Mortality										
DM	16,447	2.3	1.7	0.0	11.0	0.0	1.0	2.0	3.0	7.0
HD	64,618	8.8	3.7	0.0	33.0	2.0	6.0	8.0	11.0	19.0
CVD	91,824	12.6	4.5	2.0	47.0	4.0	9.0	12.0	15.0	25.0
RD	37,422	5.1	3.2	0.0	35.0	0.0	3.0	5.0	7.0	16.0
All causes	210,311	28.7	8.9	8.0	96.0	13.0	22.0	27.0	34.0	57.0
Meteorological										
Max. Temp.		18.5	5.5	5.4	42.0	8.6	14.4	17.8	22.1	33.7
Min. Temp.		13.4	4.2	0.2	27.6	4.5	10.2	13.5	16.8	22.8
Mean temp.		15.9	4.7	3.4	34.7	6.9	12.5	15.5	19.3	27.7
2046–2065										
Max. Temp.		20.5	5.9	7	43.6	10.5	15.8	19.7	24.5	36.4
Min. Temp.		14.9	4.4	1.8	27.8	6.9	11.3	14.7	18.3	24.9
Mean temp.		17.7	4.9	5.6	34.6	9.0	13.8	17.1	21.2	30.2

3.2. Temperature–Mortality Associations in Historical and Future Periods

3.2.1. Historical Period

Figure 1a–e (top panel) display the pooled estimates from temperature–mortality (1986–2005) curves for all-cause and cause-specific mortality. The overall mortality risks are significantly higher at lower temperatures for all-cause deaths. For example, at a temperature of 6.9 °C (1st percentile), the RR is 1.10 (95% CI: 1.01–1.19) based on an MMT of 11.1 °C (Table S1). Considering an extremely cold temperature (1st percentile) of 6.9 °C, the risk associated with RD was significant (RR = 1.33, 95% CI: 1.11–1.58) based on an MMT of 11.4 °C. By contrast, the risks associated with HD, CVD, and DM were statistically insignificant (Figure 1 and Table S1). Extreme heat (27.7 °C) was only significantly associated with RD, with an RR of 1.37 (95% CI: 1.03–1.82). The lag response from our model

for temperatures associated with 6.9 °C and 27.7 °C shows a significant, immediate, and persistent association between extremely cold temperatures and lag days. The lag response to extreme heat was statistically significant over the 21-day lag period for all cause-specific temperature–mortality relationships.

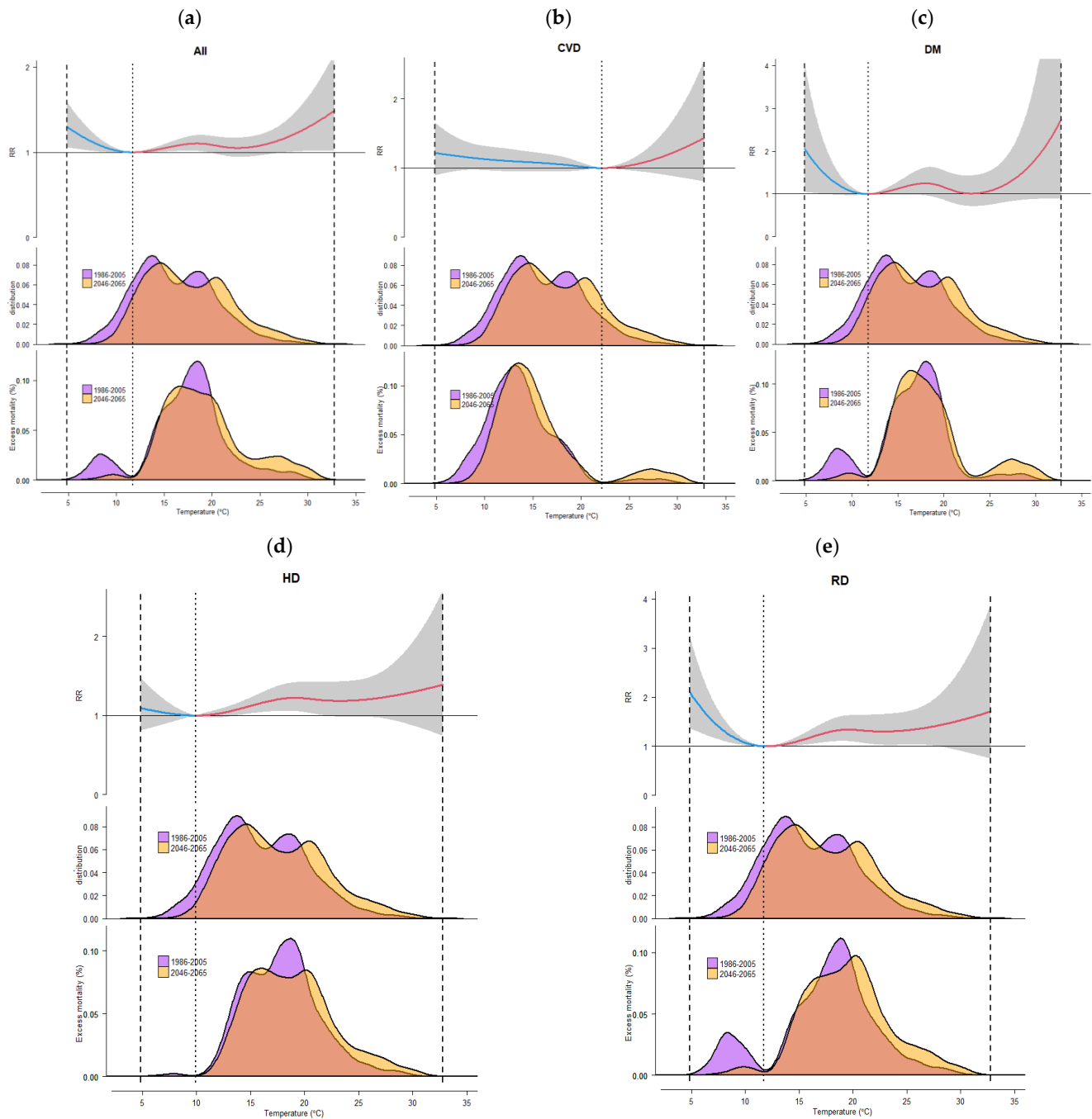


Figure 1. Temperature–mortality curves and excess mortality for the historical (1986–2005) and future (2046–2065) periods with no adaptation and population changes. (a) All-cause with MMT at 11.1 °C; (b) CVD mortality with MMT at 22.8 °C; (c) DM mortality with MMT at 11.2 °C; (d) HD mortality with MMT at 9.2 °C; (e) RD mortality with MMT at 11.4 °C. Top panel: Temperature–mortality risk curve. The middle panel represents the distribution of daily mean temperatures during the study period. The bottom panel shows the distribution of excess mortality. The dotted lines correspond to the MMT. The dashed lines indicate minimum and maximum temperatures in the historical period.

3.2.2. Future Period

The distribution of changes between the historical and future daily mean temperatures is presented in Figure S1. Daily differences (future vs. historical) in the temperature ranging from $-10.7\text{ }^{\circ}\text{C}$ to $14.6\text{ }^{\circ}\text{C}$, a median of $1.7\text{ }^{\circ}\text{C}$ (IQR: -0.5 to 3.6), and mean \pm SD (1.7 ± 3.5) were observed in this study. These findings imply a slightly warmer temperature in the future period. This is also evident in the middle panels of Figure 1a–e, which show the distribution of the temperature values in the future period superimposed on the historical period. Furthermore, the mean death counts for each day of the historical period (Figure 1) were projected to the same days of the future period (2046–2065). This ensures that the observed seasonality of death counts was preserved from the historical period to the projected future period, assuming no adverse changes in mortality distribution. Based on the methods for projected mortality data described in Section 2.3, temperature–mortality relationships for the future period were constructed considering different adaptation scenarios (with or without) and population changes (low to high fertility). The response curves in the historical period (Figure 1) indicate that the temperature–mortality association is most significant during cold periods; hence, a reduced exposure–response function (ERF) approach is not reasonable. Therefore, an absolute threshold shift of $1\text{ }^{\circ}\text{C}$ to $4\text{ }^{\circ}\text{C}$ (Reference) and three population changes (low, medium, and high fertility) were used to formulate the scenarios.

3.3. Temperature-Attributable Mortality

The distribution of excess mortality in the future period under no adaptation and population changes compared with the historical period is displayed in the bottom panel of Figure 1a–e. Figure 1 shows that the temperature–mortality attributable fraction (AF) is generally highest at cold temperatures, especially for all-cause mortality. The historical DM and RD are more pronounced than in the future period. On the other hand, the future heat-related mortality was higher than in the historical period. Table 2 shows the corresponding attributable number (AN) of excess mortalities due to non-optimum temperatures. For example, the overall all-cause temperature-related AN due to non-optimum temperatures in the historical period was 9953 (95% CI: 1294 to 17,431), extreme cold was 3263 (95% CI: 350 to 5600), and extreme heat was 2773 (95% CI: 150 to 4970). These measurements are lower than the future period, with overall all-cause temperature-related AN of 11,030 (95% CI: 730 to 20,260) and mostly due to extreme heat (AN = 9803, 95% CI: 6100 to 17,450). For different cause-specific mortality in the historical period, the AN of extreme and moderately cold weather was the highest and statistically significant for RD-related deaths at 1733 (95% CI: 720 to 2470) and 6233 (95% CI: 1750 to 10,050), respectively. For other causes of death, only HD shows significant AN for total exposure at 6373 (95% CI: 1367 to 10,451) and moderate heat at 6333 (95% CI: 1302 to 10,445). The same can be said about HD (AN = 7533, 95% CI: 1491 to 12,390) and RD (AN = 5163, 95% CI: 1646 to 7933). However, this is mostly due to moderate heat in the future period.

Table 2. Number of mortality attributable to moderate and extreme hot and cold temperatures according to cause-specific mortality and period.

Cause of Death	Period	Total	Extreme Cold	Moderate Cold	Moderate Heat	Extreme Heat
			Historical period			
All	1986–2005	9953 (1294 to 17,431)	3263 (350 to 5600)	1027 (−84 to 2005)	8923 (4270 to 16,342)	2773 (150 to 4970)
CVD	1986–2005	6401 (−2398 to 14,254)	164 (−53 to 330)	6210 (−2518 to 14,118)	191 (−187 to 490)	101 (−77 to 234)
DM	1986–2005	1577 (−604 to 3293)	60 (−5 to 101)	204 (−63 to 424)	1372 (−748 to 3056)	41 (−23 to 80)
HD	1986–2005	6373 (1367 to 10,451)	26 (−98 to 126)	45 (−221 to 269)	6333 (1302 to 10,445)	104 (−42 to 202)
RD	1986–2005	4613 (1791 to 6991)	1733 (720 to 2470)	6233 (1750 to 10,050)	3993 (1190 to 6271)	87 (−11 to 145)
			Future period			
All	2046–2065	11,030 (730 to 20,260)	22 (2 to 38)	206 (−73 to 453)	1083 (548 to 20,077)	9803 (6100 to 17,450)
CVD	2046–2065	5635 (−2343 to 12,634)	11 (−3 to 23)	5085 (−2586 to 11,977)	550 (−479 to 1345)	364 (−274 to 836)
DM	2046–2065	1621 (−921 to 3648)	4 (−0 to 7)	43 (−26 to 103)	1578 (−963 to 3645)	149 (−80 to 286)
HD	2046–2065	7533 (1491 to 12,390)	1 (−6 to 8)	4 (−27 to 31)	7523 (1478 to 12,388)	354 (−147 to 690)
RD	2046–2065	5163 (1646 to 7933)	12 (5 to 17)	1453 (110 to 2640)	5013 (1499 to 7786)	303 (−42 to 504)

Similarly, the estimated AN for future temperature-related mortality under different adaptation scenarios and population changes is presented in Table S2. The AN values vary slightly depending on whether the variable considered models with or without adaptations and/or low, medium, and high population changes. Contrary to the historical period, the estimated AN was primarily caused by warm temperatures and was non-significant in many cases. For example, when the temperature threshold was increased by 1 °C with high population changes in the future period, the estimated overall AN for all-cause mortality was 11,616.20 (95% CI: −793.27 to 22,098.15), primarily due to moderate (11,547.93, 95% CI: −913.35 to 21,976.23) and extreme heat (1445.02, 95% CI: −65.32 to 2574.79). Similar trends can be observed in other adaptation scenarios. In addition to total temperature exposure for cause-specific deaths, RD showed significant AN due to moderate cold and moderate heat across all scenarios. The total AN under a threshold of 1 °C and high RD population was 5823 (95% CI: 1797.24 to 8957.72). Moderate cold and moderate heat were 2.33 (95% CI: 1.03 to 3.45) and 5773 (95% CI: 1747.40 to 8899.93), respectively. The HD under a threshold of 1 °C and high population changes was 8683 (95% CI: 1823.10 to 14,251.99), 0.35 (95% CI: −4.30 to 4.49), and 8683 (95% CI: 1822.90 to 14,250.82) for total, moderate cold, and moderate heat, respectively. Detailed ANs for other scenarios are presented in Supplementary Table S2.

3.4. Net Differences in Excess Temperature-Related Mortality

Furthermore, we compared the net differences (change) in excess temperature-related deaths between the future and historical periods as percentage-relative AF (Figure 2). The net differences in the future temperature-related mortality relative to the historical period are displayed in Figure 2 as total, extreme, and moderate temperatures. The estimated burden for various scenarios was also presented as a percentage-relative AF in Table S3. The scenarios are classified as cause-specific (All-cause, CVD, DM, HD, RD), exposure (Total, Extreme cold, Moderate cold, Moderate heat, Extreme heat), and adaptation (None, Threshold 1 °C, Threshold 2 °C, Threshold 3 °C, Threshold 4 °C). The relative AF% (95% confidence interval) represents the adjusted fraction of temperature-related excess mortality with a 95% CI.

The results show that for all causes with total exposure and no adaptation, the total net difference for all-cause excess mortality changed by 0.53% (95% CI: −0.5% to 1.51%). However, this change was not statistically significant. Furthermore, for all causes with exposure to extreme heat and no adaptation, there was an increase of 0.33% in temperature-related excess mortality (95% CI: 0.02 to 0.59). On the other hand, cold temperatures significantly reduced mortality. For example, the significantly lower all-cause deaths in the future were attributed to extreme cold at a threshold of 1 °C and no population changes, an estimated net difference of −0.15% (95% CI: −0.26 to −0.02), a threshold of 1 °C and high population scenario of −0.15% (95% CI: −0.26 to −0.01), and a threshold of 1 °C and low population scenario of −0.15% (95% CI: −0.26 to −0.01).

Compared to the historical period for all scenarios, DM predicted a decrease in cold-related deaths and an increase in future heat-related deaths. The absence or presence of adaptation had a varying effect on the net differences between future and historical temperature-related deaths depending on the temperature exposure and adaptation type. We found that moderate cold exposure under a threshold of 1 °C and high population scenario had the greatest negative effect on relative AF% (−1.32, 95% CI: −2.65 to 0.23). In addition, moderate heat exposure under a threshold of 4 °C and high population scenario had the most positive effect at 6.75 (95% CI: −5.06 to 15.32). These net differences were mainly non-significant except for exposure to extreme cold under a threshold of 1 °C and a high population scenario (AF% = −0.38%, 95% CI: −0.63 to −0.04).

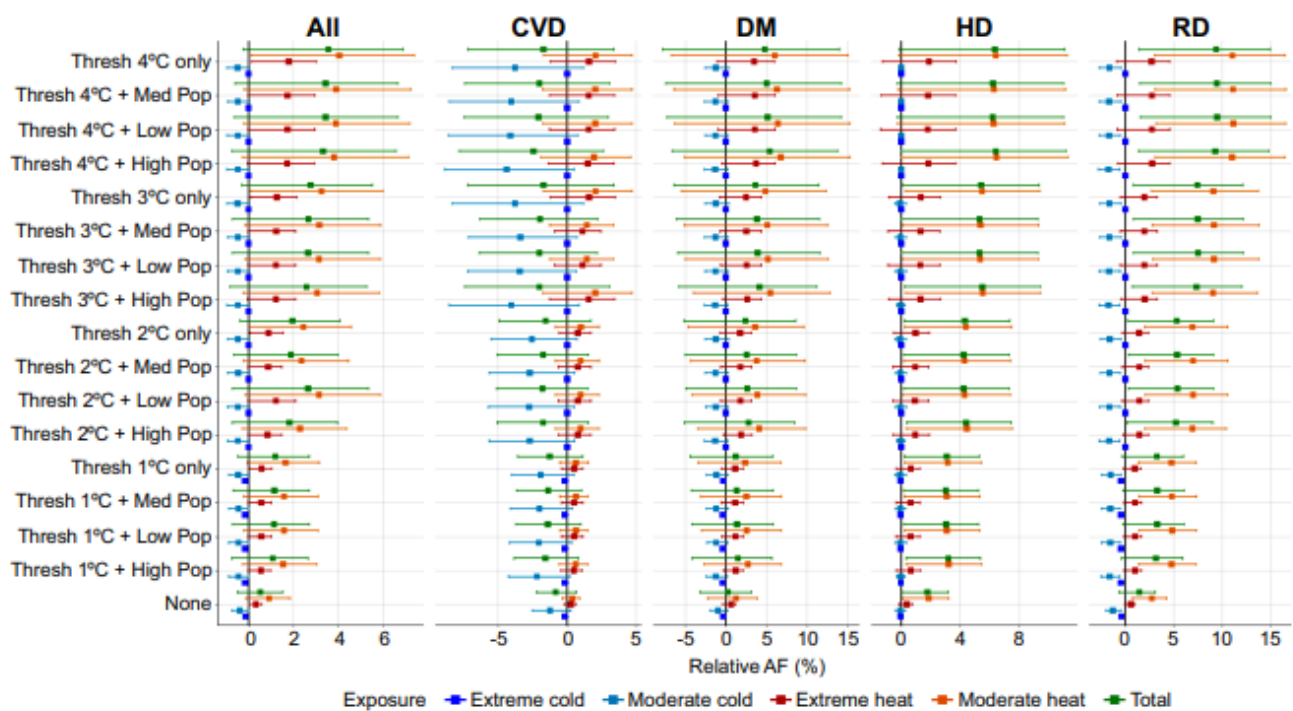


Figure 2. Net difference in excess mortality attributable to hot and cold temperatures in different adaptation scenarios and population changes. Mortality is expressed as the fraction of additional deaths (%) attributed to non-optimal temperature. CVD: cerebrovascular disease; DM: diabetes mellitus; HD: ischaemic heart disease; RD: respiratory disease; and All: all causes. The square represents the estimated difference, while the lines represent the 95% empirical confidence intervals (CIs). See Supplementary Table S3 for numerical values.

Similarly, Table S3 shows the AF% at different exposure levels and adaptation conditions for CVD. Based on different scenarios, the values represent the net difference between excess temperature-related mortality between the future and historical periods. In the scenario with no adaptation measures, the net difference in temperature-related excess mortality due to CVD is -0.83% , indicating a 0.83% decrease in deaths compared to the historical scenario. In the scenario with a threshold of $1\text{ }^{\circ}\text{C}$ only, the net difference is -1.26% , indicating a greater decrease in deaths compared to the scenario with no adaptation measures. In the scenario with a threshold of $1\text{ }^{\circ}\text{C}$ and high population density, the net difference is -1.57% , indicating an even greater decrease in deaths compared to the previous two scenarios. For extreme cold, the relative difference is -0.17% in scenarios without adaptation measures and -0.18% in scenarios with adaptation measures. Considering the threshold of $2\text{ }^{\circ}\text{C}$, the net difference in the CVD of temperature-related excess mortality for total exposure is -1.55 (-4.91 to 1.74), indicating a possible CVD mortality decrease of 1.55% (95% CI: -4.91% to 1.74%) compared to the historical data. The same scenario for moderate heat exposure shows a 1% increase in CVD mortality (95% CI: -0.83% to 2.32%).

For individuals with HD and total exposure to heat and cold, the net change in AF% without any threshold was 1.79% (95% CI: 0.04 to 3.18). The net difference in AF% for moderate heat was 1.86% (95% CI: 0.12 to 3.2) and 0.39% for extreme heat (95% CI: -0.16 to 0.76) without any threshold. The net difference for moderate cold without adaptation was -0.06% (95% CI: -0.37 to 0.3) and -0.04% for extreme cold (95% CI: -0.18 to 0.14). When a threshold of $1\text{ }^{\circ}\text{C}$ was applied, the net difference in AF% increased for total exposure (3.09% , 95% CI: 0.22 to 5.29), moderate heat (3.16% , 95% CI: 0.27 to 5.4), and extreme heat (0.66 , 95% CI: -0.31 to 1.29). For total exposure to moderate heat with a threshold of $4\text{ }^{\circ}\text{C}$ only, the net difference was 6.42% (95% CI: -0.16 to 11.27). The net difference in AF% due to HD is highest for moderate heat exposure with a threshold of $4\text{ }^{\circ}\text{C}$ only and decreases slightly with increasing levels of population adaptation.

Among the causes of death, the greatest increase in net differences in temperature-related excess death occurred in RD and was associated with heat. A significant decline in net differences was also observed in cold-related excess RD deaths. The net increase in differences increased with increasing thresholds and population sizes. For example, for RD, the net difference in extreme cold deaths was 0.46% (95% CI: -0.65 to -0.19), -1.53% for moderate cold (95% CI: -2.44 to -0.47), and 4.79% for moderate heat (95% CI: 1.34 to 7.33) under a threshold of 1 °C only and no population changes.

3.5. Model Assessment

Figure 3 presents the sensitivity results of the estimated overall cumulative temperature-mortality RR from our model at extreme cold and extreme heat to assess the robustness of the model formulation. The maximum lag varied from 21 to 28 days, and the number of df per year changed from 8 to 10 or used different temperature exposure variables, e.g., daily mean, minimum, and maximum temperatures as exposure variables. The results indicated that the varying model parameters did not substantially affect the estimated temperature-mortality coefficients. All models gave similar RRs for temperature-mortality under extreme cold and extreme heat.

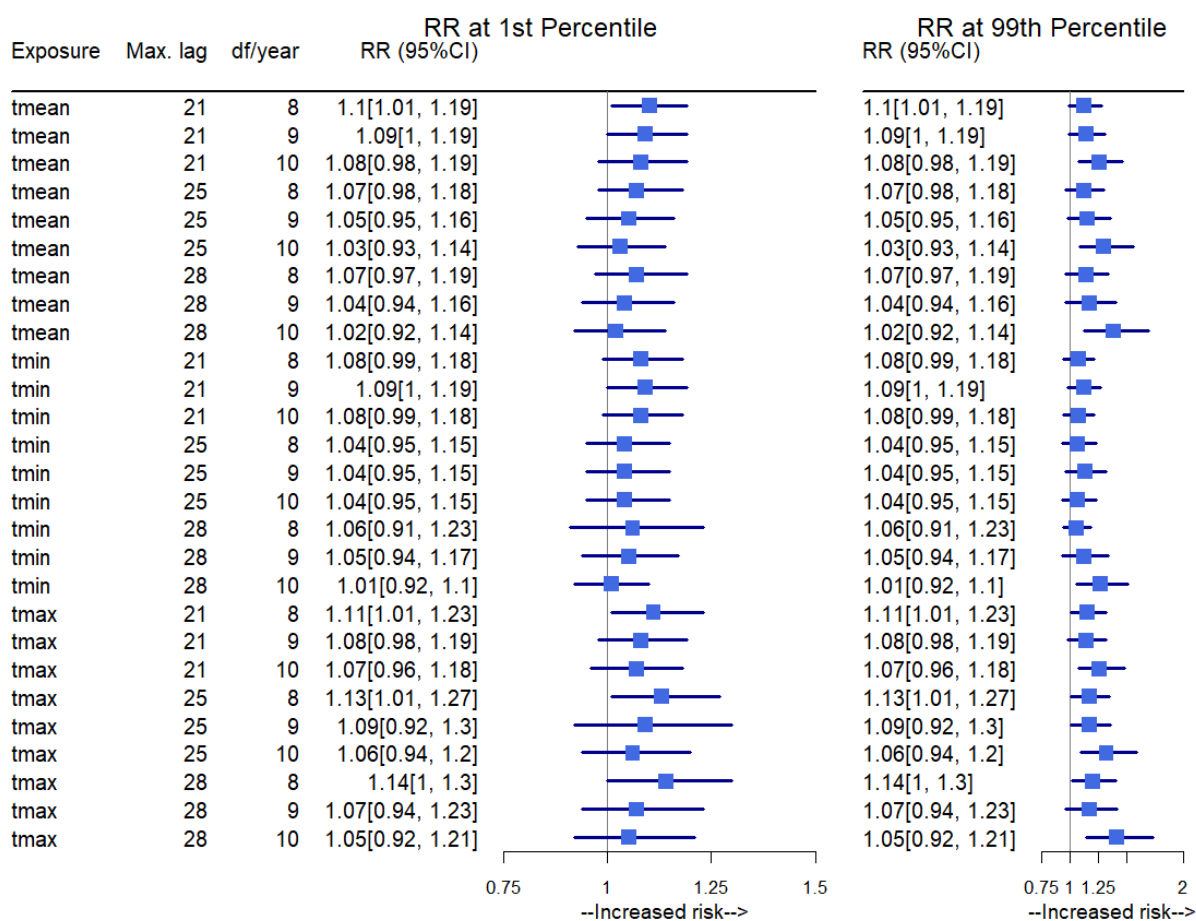


Figure 3. Sensitivity of temperature-mortality coefficient to model specification. The first column shows the different temperature variables used, and the second and third columns show each model’s maximum lag and df per year. The RR is presented for the temperature-mortality (all-cause) association in extreme cold (1st percentile) and extreme heat (99th percentile). Tmean: daily mean temperature, Tmin: daily minimum temperature, Tmax: daily maximum temperature, CI: confidence interval, max. lag: maximum lag, df: degrees of freedom.

4. Discussion

This study determined that low and high temperatures increased the mortality risk in the historical period. Cold temperatures were primarily responsible for all-cause and cause-specific deaths, particularly cerebrovascular diseases, diabetes mellitus, ischaemic heart diseases, and respiratory diseases. Historically, the attributable fraction (AF) of all specific death causes were associated with cold temperatures. These findings are generally consistent with previous studies [7,51]. In Spain, Achebak et al. [52] showed a sharp decrease in AF during the coldest months and a slight decline during the warmest months, which did not contribute to an additional decrease in cold-related deaths from respiratory disease.

According to the Organisation for Economic Co-operation and Development [53], circulatory diseases remain the leading cause of mortality in nearly all European Union (EU) member states, accounting for 7.5–8% of all deaths. As in other developed countries, the Portuguese population has progressively aged, and its fertility rate has decreased. These trends have significantly increased chronic diseases, which account for most of the disease burden. Although the Portuguese population has a longer life expectancy, it is more affected by comorbidities in advanced age (respiratory diseases, diabetes, cardiovascular diseases, obesity, and oncological conditions). This study addresses the specific concerns and needs of the Portuguese population, where chronic diseases are the leading cause of death.

Further analyses showed evidence of winter temperatures being colder in the historical period than in the future mortality period. This result was not surprising, since warmer temperatures increased during the study period. Contrary to winter temperatures, summer temperature-related deaths were significantly higher in the future period. Weinberger et al. [54] found that projected temperatures are linked with lower cold-related and higher heat-related mortality rates. Across all regions, the cold-related mortality rate per million people is projected to decrease.

This study considers the potential benefits of a warmer climate in reducing cold-related mortality. The projections indicate a reduction in cold-related deaths, historically significant causes of mortality in Lisbon. Firstly, it is crucial to acknowledge that the projected decrease in cold-related mortality may lead to substantial health and economic benefits. For example, less cold-related mortality may reduce the healthcare costs associated with cold-related illnesses and the economic costs associated with lost productivity from illness or death. Secondly, from a policy perspective, policymakers could implement several interventions to recognise the climate benefits of reduced cold-related mortality, for example, investing in infrastructure that allows vulnerable populations, such as the elderly and those with chronic respiratory illnesses, access to warm housing and efficient heating systems. Such interventions could help reduce the impact of cold weather on human health and the need for costly medical treatment. Another potential policy intervention is promoting public awareness campaigns to minimise cold exposure during winter. Such campaigns could include suitable clothing suggestions and behaviour during cold weather. They could also include advice on recognising cold-related illness symptoms and seeking appropriate medical care.

Heat-related mortality is mainly caused by chronic diseases [28]. In the future period, diabetes mellitus will be the disease most affected by high temperatures, especially mild heat. Deaths associated with high temperatures peaked in constant population projections (14.13%). In Portugal, many deaths caused by chronic conditions are avoidable. These findings have important implications for local health interventions and measurements focusing on heat and moderate extremes. Therefore, monitoring temperature is beneficial to health professionals and healthcare entities. Several studies have reported that diabetes mellitus morbidity and mortality are more susceptible to extreme temperatures, particularly heat [36,55–62].

The following limitations and strengths are acknowledged in this study. Air quality may also influence temperature variability in temperature-related mortality. However, in

this study, air quality effects were not explored. Likewise, we assumed that the future projected death rate would be similar to the annual death rate in the historical period. Although this assumption may underestimate death counts, it allows us to examine the impact of temperature-related mortality and determine whether future mortality follows a similar historical mortality pattern. We can also determine whether future projected temperatures will affect different population scenarios.

The study results suggest a relatively small increase in Lisbon's overall mortality in the late 21st century, primarily due to cold-related mortality decreases offsetting heat-related mortality increases. This projection is based on the most extreme warming scenario (RCP8.5). If we had analysed lower warming scenarios, such as RCP4.5, the increase in overall mortality might be even lower.

By using DLNM, we could model the exposure–lag–response relationship effectively. Exposure has a delayed impact that may surface over future periods. Therefore, DLNM efficiently captures and regulates the study variables' behaviour in both the exposure range and time dimension. In terms of validating smoothing techniques for exposure–lag–response relationships, this study's use of DLNM was the most effective method for modelling temperature-related mortality. Furthermore, the model was modified to consider potential variations in MMT and temperature–mortality relationships by adjusting the baseline projected population dynamics and adaptation [63,64]. This study was based on a large dataset that covered the Lisbon Metropolitan Area for all-cause and cause-specific mortality.

5. Conclusions

In summary, this study highlights the significant impact of temperature on mortality risk in Portugal, particularly for chronic diseases. It considers several population projection scenarios in the Lisbon Metropolitan Area. The findings suggest that both low and high temperatures increase mortality risk. Cold temperatures contributed to all-cause and cause-specific deaths, including cerebrovascular diseases, diabetes mellitus, ischaemic heart diseases, and respiratory diseases. By contrast, high temperatures were the main cause of future mortality, with diabetes mellitus being the most affected. In a changing climate, this study's findings and methodology have important implications for monitoring and developing targeted prevention plans for non-communicable diseases. Moreover, these findings can be used to project mortality in other regions. A deeper understanding of changes in population susceptibility will benefit local policy development in public health. This study has implications for health interventions and local-level measurements focusing on heat and moderate extremes.

Supplementary Materials: Supporting Materials can be downloaded at: <https://www.mdpi.com/article/10.3390/atmos14050775/s1>, Figure S1: Distribution of daily changes in temperature between the historical period and the future period. The blue line represents median daily temperature differences (Future vs. Historical); Table S1: MMT (SE) and RR (95% CI) at 1st (6.9 °C) and 99th (27.7 °C) percentile temperature for different cause-specific mortality; Table S2: Number of heat-related and cold-related excess mortality based on different adaptation in the future; Table S3: Net difference (Future-Historical) in temperature-related excess mortality by different scenarios (future vs. historical).

Author Contributions: Conceptualization and Design the Study, M.R.; Methodology, M.R.; Software, M.R.; Formal Analysis, M.R.; Investigation, M.R.; Data Curation, M.R.; Writing—Original Draft, M.R.; Writing—Review & Editing, M.R.; Funding Acquisition, M.R. All authors have read and agreed to the published version of the manuscript.

Funding: This study was partially supported by the Centre of Studies in Geography and Spatial Planning (CEGOT), funded by national funds through the Foundation for Science and Technology (FCT) under the reference UIDB/04084/2020; and by CESAM [UIDB/50017/2020+UIDP/50017/2020+LA/P/0094/2020] to FCT/MCTES through national funds, as well as co-funding by the FEDER, within the PT2020 Partnership Agreement and Compete 2020.

Acknowledgments: The author would like to thank the Statistics Portugal (INE—Portuguese National Institute of Statistics) for their support in obtaining the health data for this database.

Conflicts of Interest: The author declares no conflict of interest. The funders had no role in the design of the study; in the data collection, data analysis, or interpretation of data; in the writing of the manuscript, or in the decision to publish the results. The corresponding author had full access to all the data in the study.

Abbreviations

Attributable fraction	AF
Attributable number	AN
Cerebrovascular disease	CVD
Ischaemic heart disease	HD
Diabetes mellitus	DM
Respiratory diseases	RD
Lisbon Metropolitan Area	LMA
Distributed lag non-linear model	DLNM
Weather Research and Forecasting model	WRF
Exposure–response function	ERF
Relative risk	RR
Interquartile range	IQR
Minimum mortality temperature	MMT
Standard deviation	SD

References

1. Achebak, H.; Devolder, D.; Ballester, J. Trends in temperature-related age-specific and sex-specific mortality from cardiovascular diseases in Spain: A national time-series analysis. *Lancet Planet. Health* **2019**, *3*, e297–e306. [[CrossRef](#)] [[PubMed](#)]
2. Hoegh-Guldberg, O.; Jacob, D.; Taylor, M.; Bindi, M.S.; Brown, I.; Camilloni, A.; Diedhiou, R.; Djalante, K.L.; Ebi, F.; Engelbrecht, J.; et al. Impacts of 1.5 °C global warming on natural and human systems. In *Global Warming of 1.5 °C. An IPCC Special Report on the Impacts of Global Warming of 1.5 °C above Pre-Industrial Levels and Related Global Greenhouse Gas Emission Pathways, in the Context of Strengthening the Global Response to the Threat of Climate Change, Sustainable Development, and Efforts to Eradicate Poverty*; Masson-Delmotte, V., Zhai Pörtner, H.-O., Eds.; Cambridge University Press: Cambridge, UK, 2018.
3. Vicedo-Cabrera, A.M.; Sera, F.; Guo, Y.; Chung, Y.; Arbuthnott, K.; Tong, S.; Tobias, A.; Lavigne, E.; de Sousa Zanotti Stagliorio Coelho, M.; Hilario Nascimento Saldiva, P.; et al. A multi-country analysis on potential adaptive mechanisms to cold and heat in a changing climate. *Environ. Int.* **2018**, *111*, 239–246. [[CrossRef](#)] [[PubMed](#)]
4. Watts, N.; Amann, M.; Arnell, N.; Ayeb-Karlsson, S.; Beagley, J.; Belesova, K.; Boykoff, M.; Byass, P.; Cai, W.; Campbell-Lendrum, D.; et al. The 2020 report of The Lancet Countdown on health and climate change: Responding to converging crises. *Lancet* **2021**, *397*, 129–170. [[CrossRef](#)] [[PubMed](#)]
5. WHO. *Quantitative Risk Assessment of the Effects of Climate Change on Selected Causes of Death, 2030s and 2050s*; World Health Organization: Geneva, Switzerland, 2014.
6. Guo, Y.; Gasparrini, A.; Li, S.; Sera, F.; Vicedo-Cabrera, A.M.; de Sousa Zanotti Stagliorio Coelho, M.; Saldiva, P.H.N.; Lavigne, E.; Tawatsupa, B.; Punnasiri, K.; et al. Quantifying excess deaths related to heatwaves under climate change scenarios: A multicountry time series modelling study. *PLOS Med.* **2018**, *15*, e1002629. [[CrossRef](#)]
7. Li, T.; Horton, R.M.; Kinney, P. Future projections of seasonal patterns in temperature-related deaths for Manhattan. *Nat. Clim. Chang.* **2013**, *3*, 717–721. [[CrossRef](#)]
8. Martínez-Solanas, È.; Quijal-Zamorano, M.; Achebak, H.; Petrova, D.; Robine, J.M.; Herrmann, F.R.; Rodó, X.; Ballester, J. Projections of temperature-attributable mortality in Europe: A time series analysis of 147 contiguous regions in 16 countries. *Lancet Planet. Health* **2021**, *5*, e446–e454. [[CrossRef](#)]
9. Smith, K.R.; Woodward, A.; Campbell-Lendrum, D.; Chadee, D.D.; Honda, Y.; Liu, Q.; Olwoch, J.M.; Revich, B.; Sauerborn, R. Human health: Impacts, adaptation, and co-benefits. In *Climate Change 2014: Impacts, Adaptation, and Vulnerability. Part A: Global and Sectoral Aspects. Contribution of Working Group II to the Fifth Assessment Report of the Intergovernmental Panel of Climate Change*; Field, C.B., Barros, V.R., Dokken, D.J., Mach, K.J., Mastrandrea, M.D., Bilir, T.E., Chatterjee, M., Ebi, K.L., Estrada, Y.O., Genova, R.C., et al., Eds.; Cambridge University Press: Cambridge, UK, 2014; pp. 709–754.
10. Costello, A.; Abbas, M.; Allen, A.; Ball, S.; Bell, S.; Bellamy, R.; Friel, S.; Groce, N.; Johnson, A.; Kett, M.; et al. Managing the health effects of climate change: Lancet and University College London Institute for Global Health Commission. *Lancet* **2009**, *373*, 1693–1733. [[CrossRef](#)] [[PubMed](#)]
11. Ebi, K.L.; Ogden, N.H.; Semenza, J.C.; Woodward, A. Detecting and attributing health burdens to climate change. *Environ. Health Perspect.* **2017**, *125*, 085004. [[CrossRef](#)]

12. Ebi, K.; Prats, E. Health in national climate change adaptation planning. *Ann. Glob. Health* **2015**, *81*, 418–426. [[CrossRef](#)] [[PubMed](#)]
13. Son, J.Y.; Liu, J.C.; Bell, M.L. Temperature-related mortality: A systematic review and investigation of effect modifiers. *Environ. Res. Lett.* **2019**, *14*, 073004. [[CrossRef](#)]
14. Rodrigues, M.; Santana, P.; Rocha, A. Modelling of Temperature-Attributable Mortality among the Elderly in Lisbon Metropolitan Area, Portugal: A Contribution to Local Strategy for Effective Prevention Plans. *J. Urban Health* **2021**, *98*, 516–531. [[CrossRef](#)]
15. Yin, P.; Chen, R.; Wang, L.; Liu, C.; Niu, Y.; Wang, W.; Jiang, Y.; Liu, Y.; Liu, J.; Qi, J.; et al. The added effects of heatwaves on cause-specific mortality: A nationwide analysis in 272 Chinese cities. *Environ. Int.* **2018**, *121*, 898–905. [[CrossRef](#)] [[PubMed](#)]
16. Petkova, E.; Horton, R.; Bader, D.; Kinney, P. Projected heat-related mortality in the U.S. urban northeast. *Int. J. Environ. Res. Public Health* **2013**, *10*, 6734–6747. [[CrossRef](#)] [[PubMed](#)]
17. Rodrigues, M.; Santana, P.; Rocha, A. Modelling climate change impacts on attributable-related deaths and demographic changes in the largest metropolitan area in Portugal: A time-series analysis. *Environ. Res.* **2020**, *190*, 109998. [[CrossRef](#)] [[PubMed](#)]
18. Navas-Martín, M.; López-Bueno, J.A.; Díaz, J.; Follos, F.; Vellón, J.; Mirón, I.; Luna, M.; Sánchez-Martínez, G.; Culqui, D.; Linares, C. Effects of local factors on adaptation to heat in Spain (1983–2018). *Environ. Res.* **2022**, *209*, 112784. [[CrossRef](#)]
19. Cole, R.; Hajat, S.; Murage, P.; Heaviside, C.; Macintyre, H.; Davies, M.; Wilkinson, P. The contribution of demographic changes to future heat-related health burdens under climate change scenarios. *Environ. Int.* **2023**, *173*, 107836. [[CrossRef](#)]
20. Armstrong, B.; Bell, M.L.; de Sousa Zanotti Stagliorio Coelho, M.; Leon Guo, Y.L.; Guo, Y.; Goodman, P.; Hashizume, M.; Honda, Y.; Kim, H.; Lavigne, E.; et al. Longer-term impact of high and low temperature on mortality: An international study to clarify length of mortality displacement. *Environ. Health Perspect.* **2017**, *125*, 107009. [[CrossRef](#)]
21. Mitchell, D. Human influences on heat-related health indicators during the 2015 Egyptian heat wave. *Bull. Am. Meteorol. Soc.* **2016**, *97*, S70–S74. [[CrossRef](#)]
22. Vicedo-Cabrera, A.M.; Scovronick, N.; Sera, F.; Roye, D.; Schneider, R.; Tobias, A.; Astrom, C.; Guo, Y.; Honda, Y.; Hondula, D.M.; et al. The burden of heat-related mortality attributable to recent human-induced climate change. *Nat. Clim. Chang.* **2021**, *11*, 492–500. [[CrossRef](#)]
23. IPCC. Intergovernmental panel on climate change. In *Climate Change 2022: Impacts, Adaptation, and Vulnerability*; Contribution of Working Group II to the Sixth Assessment Report of the Intergovernmental Panel on Climate Change; Pörtner, H.-O., Roberts, D.C., Tignor, M., Poloczanska, E.S., Mintenbeck, K., Alegria, A., Craig, M., Langsdorf, S., Lösschke, S., Möller, V., et al., Eds.; Cambridge University Press: Cambridge, UK; New York, NY, USA, 2022; p. 3056. [[CrossRef](#)]
24. EPA. United Environmental Protection Agency. Climate Change and Heat Islands. 2022. Available online: <https://www.epa.gov/heatislands/climate-change-and-heat-islands> (accessed on 18 January 2023).
25. WHO. *Zero Regrets: Scaling Up Action on Climate Change Mitigation and Adaptation for Health in the WHO European Region. Key Messages from the Working Group on Health in Climate Change*; World Health Organization, Regional Office for Europe: Copenhagen, Denmark, 2021; Available online: <https://apps.who.int/iris/handle/10665/344733> (accessed on 18 January 2023).
26. Tong, S.; Ebi, K. Preventing and mitigating health risks of climate change. *Environ. Res.* **2019**, *174*, 9–13. [[CrossRef](#)]
27. Breil, M.; Downing, C.; Kazmierczak, A.; Mäkinen, K.; Romanovska, L. *Social Vulnerability to Climate Change in European Cities—State of Play in Policy and Practice*; European Topic Centre on Climate Change Impacts, Vulnerability and Adaptation (ETC/CCA) Technical Paper 2018/1; ETC/CCA: Bologna, Italy, 2018. [[CrossRef](#)]
28. Ellena, M.; Ballester, J.; Mercogliano, P.; Ferracin, E.; Barbato, G.; Costa, G.; Ingoles, V. Social inequalities in heat-attributable mortality in the city of Turin, northwest of Italy: A time series analysis from 1982 to 2018. *Environ. Health* **2020**, *19*, 116. [[CrossRef](#)] [[PubMed](#)]
29. Ebi, K.; Campbell-Lendrum, D.; Wyns, A. The 1.5 Health Report: Synthesis on Health & Climate Science in the IPCC SR1.5. Available online: <https://www.who.int/publications/i/item/the-1.5-health-report> (accessed on 6 January 2023).
30. Ebi, K.L.; Capon, A.; Berry, P.; Broderick, C.; de Dear, R.; Havenith, G.; Honda, Y.; Kovats, R.S.; Ma, W.; Malik, A.; et al. Hot Weather and Heat Extremes: Health Risks. *Lancet* **2021**, *398*, 698–708. [[CrossRef](#)] [[PubMed](#)]
31. Pascal, M.; Wagner, V.; Corso, M.; Laaidi, K.; Ung, A.; Beaudeau, P. Heat and cold related-mortality in 18 French cities. *Environ. Int.* **2018**, *121*, 189–198. [[CrossRef](#)] [[PubMed](#)]
32. Kenny, G.P.; Yardley, J.; Brown, C.; Sigal, R.J.; Jay, O. Heat stress in older individuals and patients with common chronic diseases. *CMAJ* **2010**, *182*, 1053–1060. [[CrossRef](#)] [[PubMed](#)]
33. Schneider, A.; Rückel, R.; Breitner, S.; Wolf, K.; Peters, A. Thermal Control, Weather, and Aging. *Curr. Environ. Health Rep.* **2017**, *4*, 21–29. [[CrossRef](#)]
34. Martinez, G.S.; Diaz, J.; Hooyberghs, H.; Lauwaet, D.; De Ridder, K.; Linares, C.; Carmona, R.; Ortiz, C.; Kendrovski, V.; Adamonyte, D. Cold-related mortality vs heat-related mortality in a changing climate: A case study in Vilnius (Lithuania). *Environ. Res.* **2018**, *166*, 384–393. [[CrossRef](#)] [[PubMed](#)]
35. Weitensfelder, L.; Moshammer, H. Evidence of adaptation to increasing temperatures. *Int. J. Environ. Res. Public Health* **2020**, *17*, 97. [[CrossRef](#)]
36. Hajat, S. Health effects of milder winters: A review of evidence from the United Kingdom. *Environ. Health* **2017**, *16*, 109. [[CrossRef](#)]

37. Diaz, J.; Carmona, R.; Miron, I.J.; Luna, M.Y.; Linares, C. Time trends in the impact attributable to cold days in Spain: Incidence of local factors. *Sci. Total Environ.* **2019**, *655*, 305–312. [[CrossRef](#)]
38. Burkart, K.; Meier, F.; Schneider, A.; Breitner, S.; Canário, P.; Alcoforado, M.J.; Scherer, D.; Endlicher, W. Modification of heat-related mortality in an elderly urban population by vegetation (urban green) and proximity to water (urban blue): Evidence from Lisbon, Portugal. *Environ. Health Perspect.* **2016**, *124*, 927–934. [[CrossRef](#)]
39. Sillmann, J.; Kharin, V.V.; Zwiers, F.W.; Zhang, X.; Bronaugh, D. Climate extremes indices in the CMIP5 multimodel ensemble: Part 2. Future climate projections. *J. Geophys. Res. Atmos.* **2013**, *118*, 2473–2493. [[CrossRef](#)]
40. Pereira, S.C.; Marta-Almeida, M.; Carvalho, A.C.; Rocha, A. Heat wave and cold spell changes in Iberia for a future climate scenario. *Int. J. Clim.* **2017**, *37*, 5192–5205. [[CrossRef](#)]
41. Fonseca, D.; Carvalho, M.J.; Marta-Almeida, M.; Melo-Gonçalves, P.; Rocha, A. Recent trends of extreme temperature indices for the Iberian Peninsula. *Phys. Chem. Earth* **2016**, *94*, 66–76. [[CrossRef](#)]
42. Gasparrini, A.; Leone, M. Attributable risk from distributed lag models. *BMC Med. Res. Methodol.* **2014**, *14*, 55. [[CrossRef](#)]
43. Gasparrini, A. Distributed lag linear and non-linear models in R: The package dlnm. *J. Stat. Softw.* **2011**, *43*, 1. [[CrossRef](#)]
44. Rodrigues, M.; Natário, I.; do Rosário de Oliveira Martins, M. Estimate the effects of environmental determining factors on childhood asthma hospital admissions in Lisbon, Portugal: A time series modelling study. *Theor. Appl. Climatol.* **2021**, *143*, 809–821. [[CrossRef](#)]
45. Rodrigues, M.; Santana, P.; Rocha, A. Effects of extreme temperatures on cerebrovascular mortality in Lisbon: A distributed lag non-linear model. *Int. J. Biometeorol.* **2019**, *63*, 549–559. [[CrossRef](#)]
46. Gasparrini, A.; Guo, Y.; Hashizume, M.; Kinney, P.; Petkova, E.P.; Lavigne, E.; Zanobetti, A.; Schwartz, J.; Tobias, A.; Leone, M.; et al. Temporal variation in heat–mortality associations: A multicountry study. *Environ. Health Perspect.* **2015**, *123*, 1200–1207. [[CrossRef](#)]
47. Scovronick, N.; Sera, F.; Acquafredda, F.; Garzena, D.; Fratianni, S.; Wright, C.Y.; Gasparrini, A. The association between ambient temperature and mortality in South Africa: A time-series analysis. *Environ. Res.* **2018**, *161*, 229–235. [[CrossRef](#)]
48. Gasparrini, A.; Guo, Y.; Sera, F.; Vicedo-Cabrera, A.M.; Huber, V.; Tong, S.; Coelho, M.D.; Saldiva, P.H.; Lavigne, E.; Correa, P.M.; et al. Projections of temperature-related excess mortality under climate change scenarios. *Lancet Planet. Health* **2017**, *1*, e360–e367. [[CrossRef](#)]
49. Yang, J.; Zhou, M.; Ren, Z.; Li, M.; Wang, B.; Li Liu, D.; Ou, C.-Q.; Yin, P.; Sun, J.; Tong, S. Projecting heat-related excess mortality under climate change scenarios in China. *Nat. Commun.* **2021**, *12*, 1039. [[CrossRef](#)] [[PubMed](#)]
50. Gosling, S.N.; Hondula, D.M.; Bunker, A.; Ibarreta, D.; Liu, J.; Zhang, X.; Sauerborn, R. Adaptation to climate change: A comparative analysis of modeling methods for heat-related mortality. *Environ. Health Perspect.* **2017**, *125*, 087008. [[CrossRef](#)] [[PubMed](#)]
51. Guo, Y.; Li, S.; Liu, D.L.; Chen, D.; Williams, G.; Tong, S. Projecting future temperature-related mortality in three largest Australian cities. *Environ. Pollut.* **2016**, *208*, 66–73. [[CrossRef](#)] [[PubMed](#)]
52. Achebak, H.; Devolder, D.; Ingole, V.; Ballester, J. Reversal of the seasonality of temperature-attributable mortality from respiratory diseases in Spain. *Nat. Commun.* **2020**, *11*, 2457. [[CrossRef](#)] [[PubMed](#)]
53. OECD/European Union. *Health at a Glance: Europe 2020: STATE of Health in the EU Cycle*; OECD Publishing: Paris, France, 2020. [[CrossRef](#)]
54. Weinberger, K.R.; Haykin, L.; Eliot, M.N.; Schwartz, J.D.; Gasparrini, A.; Wellenius, G.A. Projected temperature-related deaths in ten large U.S. metropolitan areas under different climate change scenarios. *Environ. Int.* **2017**, *107*, 196–204. [[CrossRef](#)] [[PubMed](#)]
55. Lavigne, E.; Gasparrini, A.; Wang, X.; Chen, H.; Yagouti, A.; Fleury, M.D.; Cakmak, S. Extreme ambient temperatures and cardiorespiratory emergency room visits: Assessing risk by comorbid health conditions in a time series study. *Environ. Health* **2014**, *13*, 5. [[CrossRef](#)]
56. Schwartz, J. Who is Sensitive to Extremes of Temperature? A Case-Only Analysis. *Epidemiology* **2005**, *16*, 67–72. [[CrossRef](#)]
57. Åström, D.O.; Schifano, P.; Asta, F.; Lallo, A.; Michelozzi, P.; Rocklöv, J.; Forsberg, B. The effect of heat waves on mortality in susceptible groups: A cohort study of a Mediterranean and a northern European City. *Environ. Health* **2015**, *14*, 30. [[CrossRef](#)]
58. Ma, Y.; Zhou, L.; Chen, K. Burden of cause-specific mortality attributable to heat and cold: A multicity time-series study in Jiangsu Province, China. *Environ. Int.* **2020**, *2020*, 144105994. [[CrossRef](#)]
59. Li, Y.; Lan, L.; Wang, Y.; Yang, C.; Tang, W.; Cui, G.; Luo, S.; Cheng, Y.; Liu, Y.; Liu, J.; et al. Extremely cold and hot temperatures increase the risk of diabetes mortality in metropolitan areas of two Chinese cities. *Environ. Res.* **2014**, *134*, 91–97. [[CrossRef](#)]
60. Yardley, J.E.; Stapleton, J.M.; Sigal, R.J.; Kenny, G.P. Do heat events pose a greater health risk for individuals with type 2 diabetes? *Diabetes Technol. Ther.* **2013**, *15*, 520–529. [[CrossRef](#)] [[PubMed](#)]
61. Medina-Ramón, M.; Schwartz, J. Temperature, temperature extremes, and mortality: A study of acclimatisation and effect modification in 50 US cities. *Occup. Environ. Med.* **2007**, *64*, 827–833. [[CrossRef](#)] [[PubMed](#)]
62. Basu, R.; Samet, J.M. Relation between elevated ambient temperature and mortality: A review of the epidemiologic evidence. *Epidemiol. Rev.* **2002**, *24*, 190–202. [[CrossRef](#)] [[PubMed](#)]

63. Sierra, F.; Hadley, E.; Suzman, R.; Hodes, R. Prospects for life span extension. *Annu. Rev. Med.* **2009**, *60*, 457–469. [[CrossRef](#)] [[PubMed](#)]
64. Åström, D.O.; Tornevi, A.; Ebi, K.L.; Rocklöv, J.; Forsberg, B. Evolution of minimum mortality temperature in Stockholm, Sweden, 1901–2009. *Environ. Health Perspect.* **2016**, *124*, 740–744. [[CrossRef](#)]

Disclaimer/Publisher’s Note: The statements, opinions and data contained in all publications are solely those of the individual author(s) and contributor(s) and not of MDPI and/or the editor(s). MDPI and/or the editor(s) disclaim responsibility for any injury to people or property resulting from any ideas, methods, instructions or products referred to in the content.